Hong Kong J Radiol. 2026;29:Epub. Published 6 March 2026 | https://doi.org/10.12809/hkjr2518018

PICTORIAL ESSAY

Revisiting Preoperative Evaluation of the Inferior Vena Cava in Abdominal Malignancies: A Pictorial Essay

A Mandava[1], V Koppula[1], M Kandati[1], AK Reddy[1], H Kacharagadla[1], SR Thammineedi[2]

[1]Department of Radiodiagnosis, Basavatarakam Indo American Cancer Hospital and Research Institute, Hyderabad, India

[2]Department of Surgical Oncology, Basavatarakam Indo American Cancer Hospital and Research Institute, Hyderabad, India

INTRODUCTION

Inferior vena cava (IVC) is the largest vein in the body, draining blood from the lower extremities, pelvis, and abdomen into the right atrium. Accurate anatomical assessment is crucial when planning vascular interventions, resections, anastomoses, and reconstructions that form an integral part of the surgical management of abdominopelvic malignancies. Anomalies and variants can complicate access to the IVC and its tributaries during interventional procedures and filter placement. Given that abdominopelvic oncological surgeries require extensive dissections, unawareness of vascular involvement and congenital anomalies can lead to inadvertent injuries with catastrophic outcomes. Contrast-enhanced computed tomography with reconstruction is the gold-standard non-invasive investigation for presurgical mapping; ultrasound with colour Doppler, magnetic resonance imaging, and positron emission tomography/computed tomography often play complementary roles in evaluating the IVC and its draining veins. This pictorial essay presents several illustrative cases from our experience at a tertiary care cancer centre in India.

ANATOMY AND VARIANTS

The embryogenesis and development of the IVC is a complex process, and multiple congenital variations can arise from abnormal persistence or regression of embryological veins (Table 1).[1-8] These congenital anomalies are collectively present in 4% of the population.[2-8] The most common clinically significant variations include duplication of the IVC and absence or agenesis (interruption) of the IVC with prominent hemiazygos-azygos pathways[2] (Figures 1 to 5). Because

Correspondence: *Dr A Mandava, Department of Radiodiagnosis, Basavatarakam Indo American Cancer Hospital and Research Institute, Hyderabad, India*
Email: dranitha@basavatarakam.org

Submitted: 6 August 2025; Accepted: 23 November 2025. This version may differ from the final version when published in an issue.

Contributors: All authors designed the study, acquired the data, analysed the data, drafted the manuscript, and critically revised the manuscript for important intellectual content. All authors had full access to the data, contributed to the study, approved the final version for publication, and take responsibility for its accuracy and integrity.

Conflicts of Interest: All authors have disclosed no conflicts of interest.

Funding/Support: This study received no specific grant from any funding agency in the public, commercial, or not-for-profit sectors.

Data Availability: All data generated or analysed during the present study are available from the corresponding author on reasonable request.

Ethics Approval: The study was approved by the Institutional Ethics Committee of Basavatarakam Indo American Cancer Hospital and Research Institute, India (Ref No.: IEC/2021/55). A waiver of informed patient consent was granted by the Committee as the study involved minimal risk and non-identifiable data were used.

Declaration: A few of the images were presented as part of scientific exhibit in Radiological Society of North America Annual Meeting 2023, Chicago [IL], United States, 26-30 November 2023.

visceral thoracic and abdominal organs demonstrate left-right anatomical asymmetry, awareness of discrepancies in laterality and venous drainage into the IVC—such as in situs inversus and heterotaxy syndromes—is critical before undertaking biliary, hepatic, and gastric surgeries (Figure 6). Variations in renal vein anatomy are often asymptomatic and overlooked but are crucial during renal or adrenal surgeries and retroperitoneal dissections. Anomalous veins and collateral vessels may be misdiagnosed as lymphadenopathy; hence, contrast imaging is essential in all cases of malignancy (Figures 7 to 9).

Table 1. Common congenital anomalies involving the inferior vena cava and their incidence.[1-8]

	Incidence
Agenesis of IVC	0.0005% to 1%
Duplication of IVC	0.2% to 3.0%
Left-sided IVC	0.2% to 0.5%
Retroaortic left renal vein	1.2% to 2.4%
Circumaortic left renal vein	1.5% to 8.7%
Situs inversus totalis	0.01%

Abbreviation: IVC = inferior vena cava.

ACQUIRED PATHOLOGIES

The major acquired venous pathologies in abdominopelvic malignancies include external compression or infiltration of the IVC and its draining veins by neoplasms (Figures 10 and 11), metastatic lymph nodes (Figure 12), and/or intraluminal thrombosis.

Malignancies most commonly involving the IVC include those of the liver (4.0%-5.9%), kidney (4%-10%), and adrenal glands (9%-19%).[4,8] Although the portal veins are more frequently involved, abnormalities of the hepatic artery, hepatic veins, and IVC may occur in hepatocellular carcinomas; accordingly, triphasic computed tomography should be performed in the evaluation of liver malignancies (Figure 13).

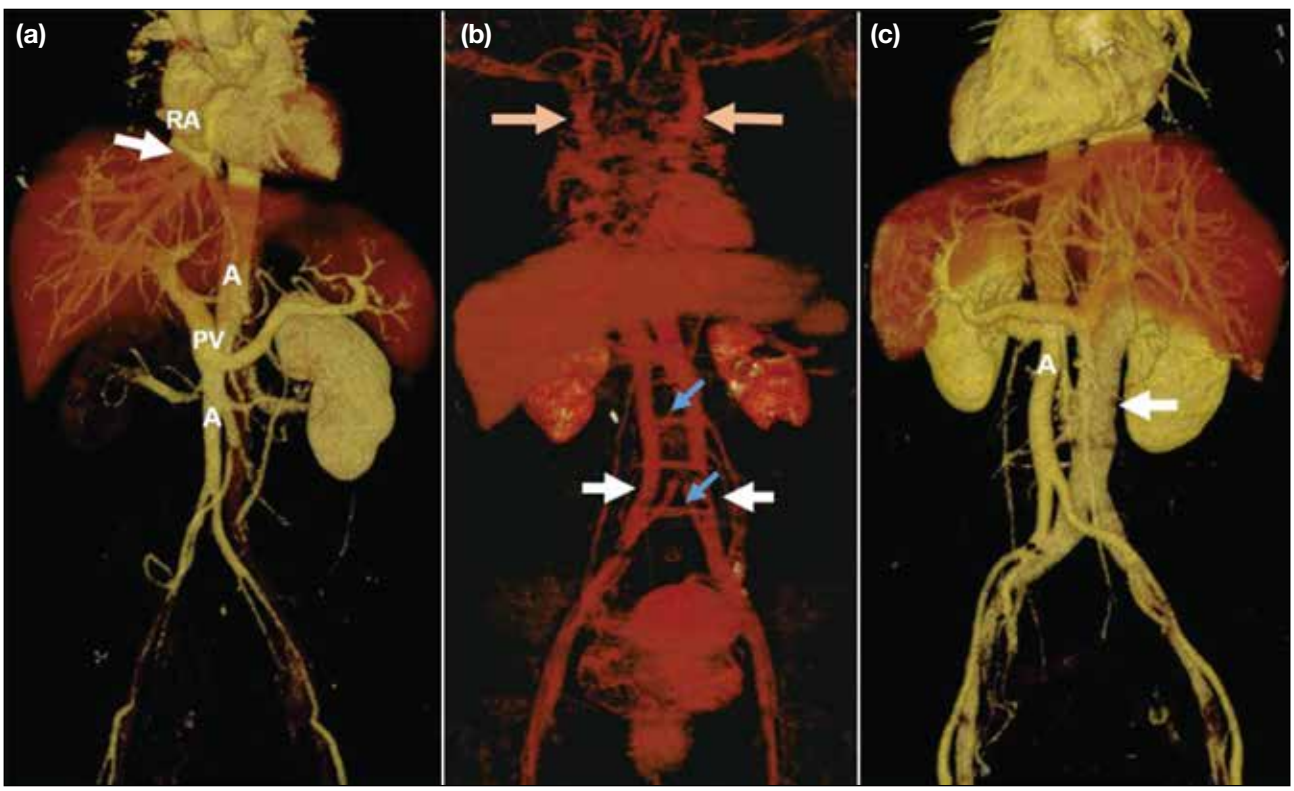

Figure 1. Volume-rendered contrast-enhanced computed tomography images. (a) Interrupted inferior vena cava (IVC) with absence of the infrahepatic IVC. The suprahepatic IVC (white arrow) drains into the right atrium (RA) of the heart. The normal portal vein (PV) and the aorta (A) are visible. (b) Rare case of complete duplication of the superior vena cava in the thorax (orange arrows) and the IVC in the abdomen (white arrows), with multiple bridging veins between duplicated segments (blue arrows). (c) The IVC (white arrow) lies to the left of the aorta (A), with dextrocardia in a patient with situs inversus totalis.

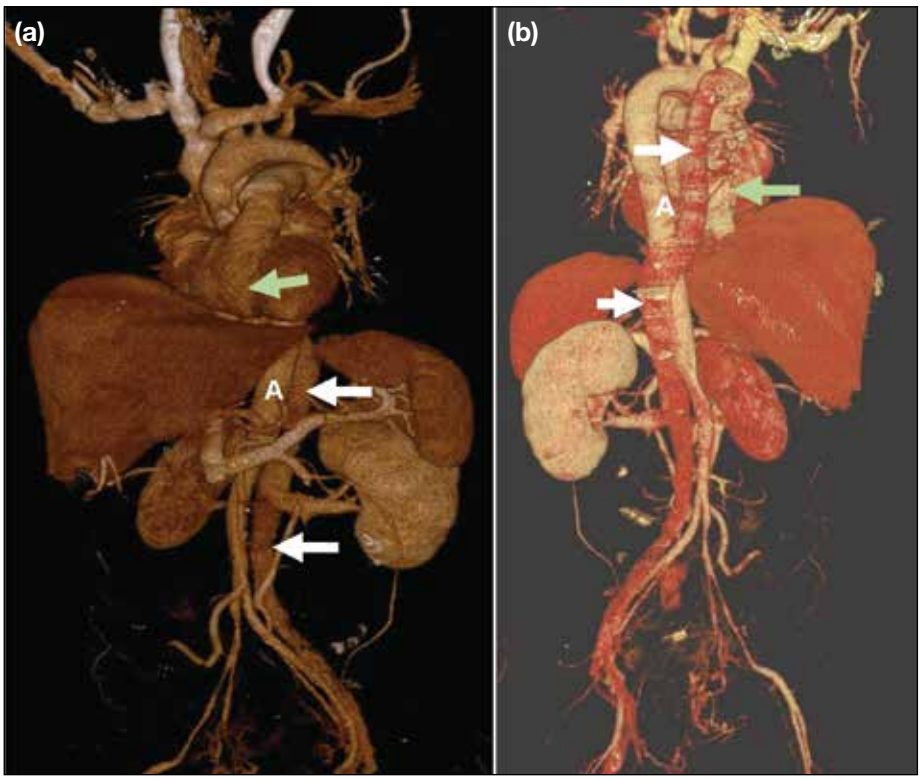

Figure 2. (a) Anterior and (b) posterior volume-rendered contrast-enhanced computed tomography images show a left inferior vena cava with hemiazygos continuation, crossing the midline posterior to the aorta (A) and draining into the azygos-superior vena cava pathway (white arrows). Hepatic veins are visible draining separately into the right atrium (green arrows).

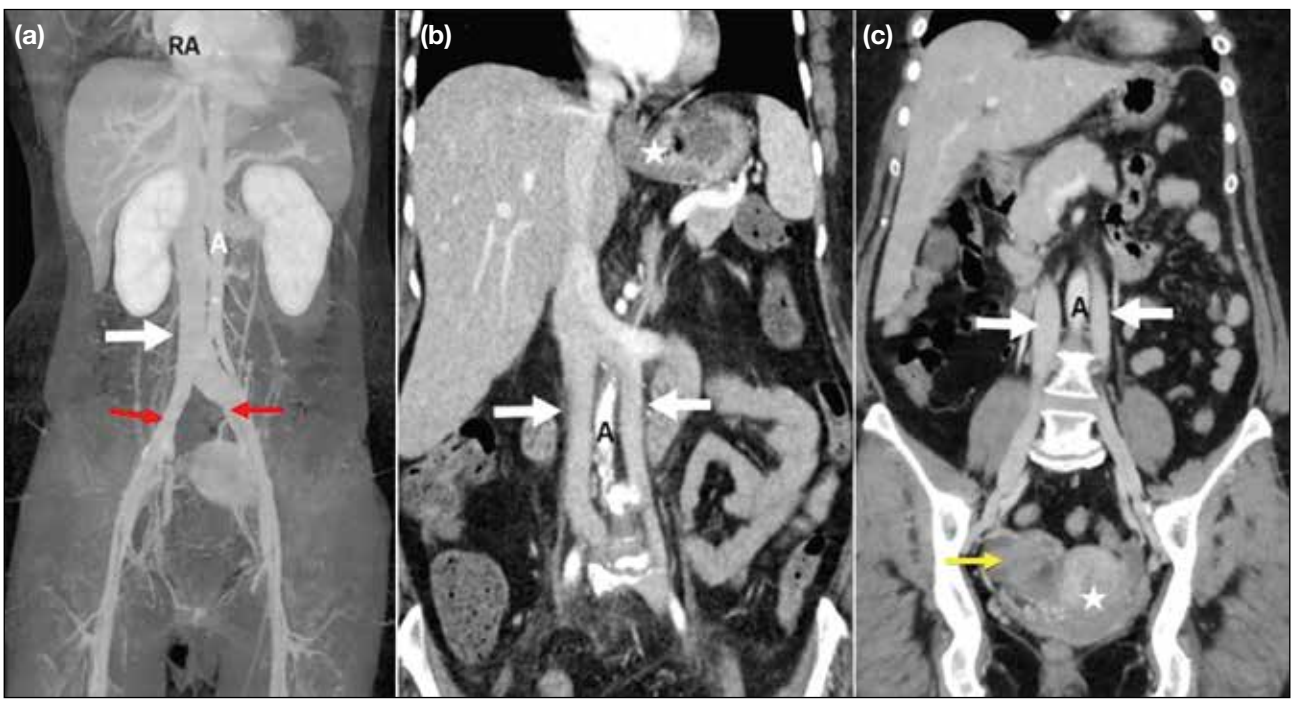

Figure 3. Coronal maximum intensity projection contrast-enhanced computed tomography images of the abdomen. (a) Normal inferior vena cava (IVC) [white arrow] to the right of the aorta (A), formed by the confluence of the bilateral common iliac veins (red arrows), draining into the right atrium (RA). (b) Duplication of the IVC (white arrows) in a patient with gastric malignancy (star). The left infrarenal IVC crosses the midline anterior to the aorta (A) and joins the right IVC. (c) Duplication of the IVC (white arrows) on both sides of the aorta (A) in a patient with endometrial malignancy (star) and a complex right ovarian cyst (yellow arrow).

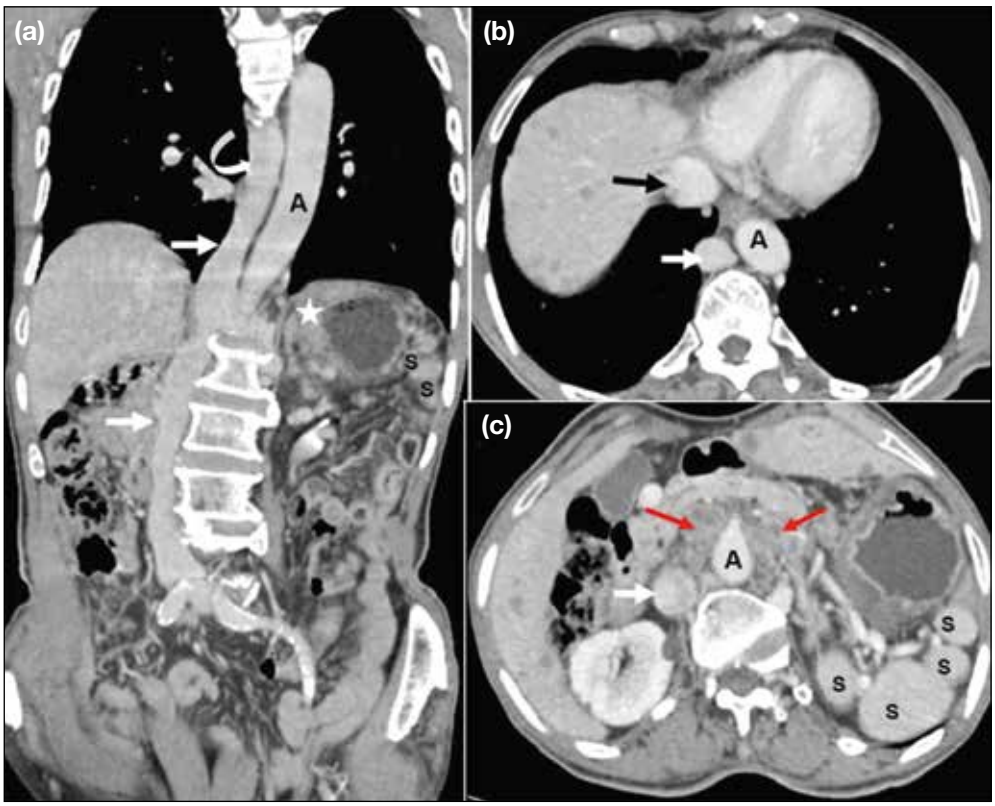

Figure 4. Coronal (a) and axial (b, c) contrast-enhanced computed tomography images in a patient with gastric malignancy (star) show polysplenia (S) and a right inferior vena cava with azygos continuation (white arrows) draining into the superior vena cava (curved arrow in [a]). Hepatic veins drain separately into the right atrium (black arrow in [b]), and para-aortic lymphadenopathy is also noted (red arrows in [c]).
Abbreviation: A = aorta.

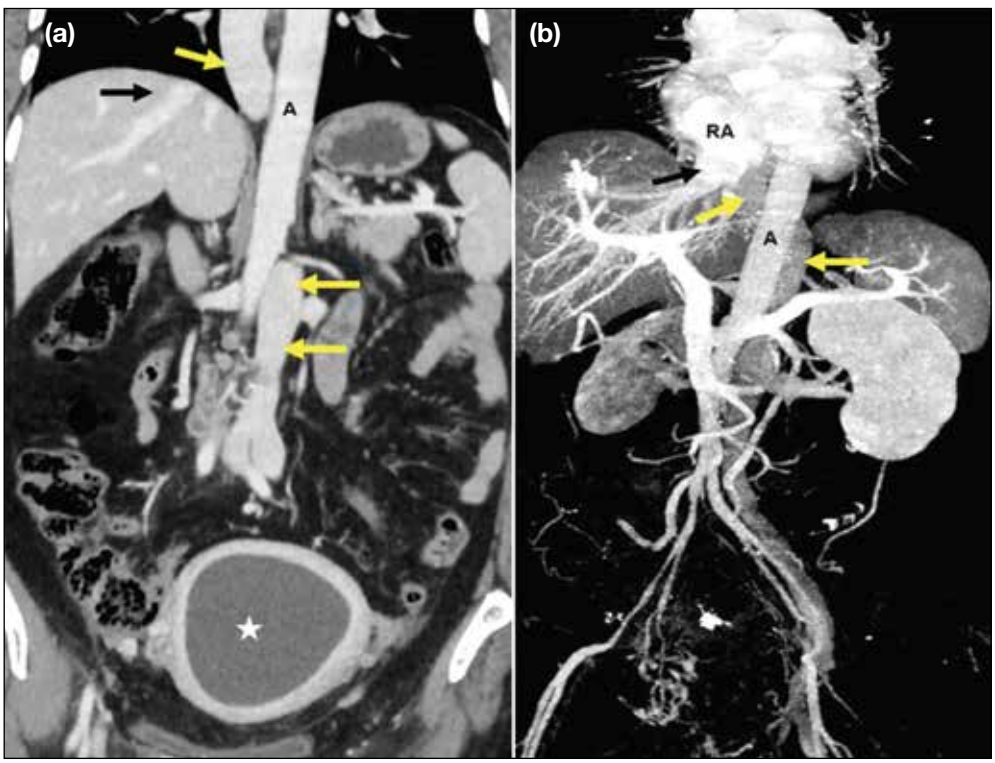

Figure 5. (a) Coronal contrast-enhanced computed tomography and (b) posterior maximum intensity projection images of a patient with cervical carcinoma and pyometra (star in [a]) show a left inferior vena cava crossing the midline posterior to the aorta (A), continuing as the azygos-superior vena cava pathway (yellow arrows). Hepatic veins (black arrows) drain separately into the right atrium (RA).

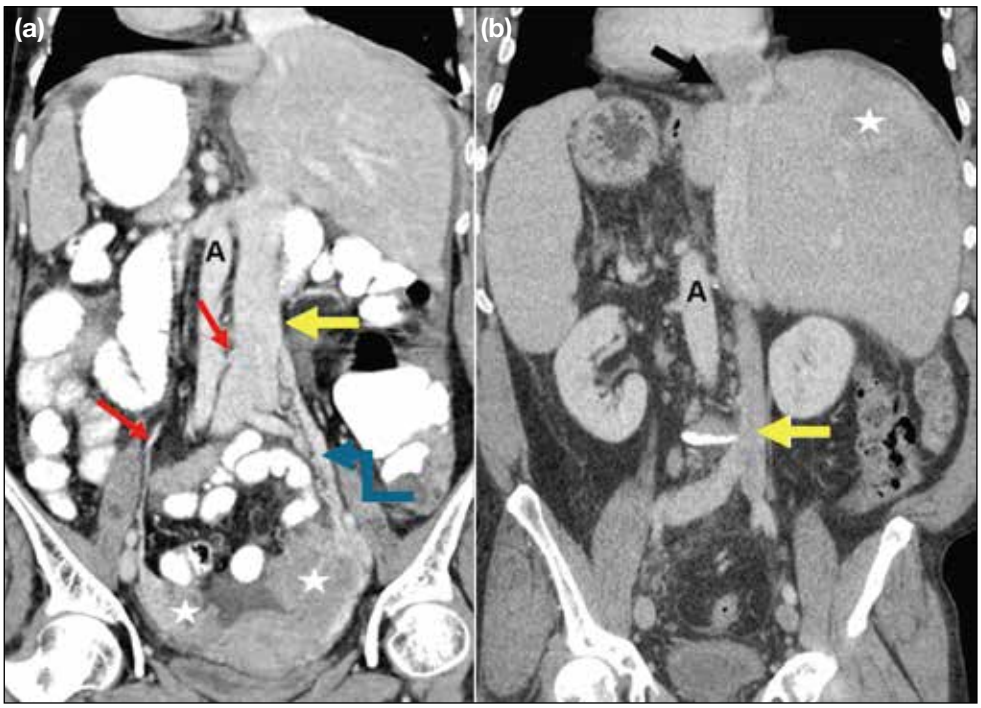

Figure 6. Two cases of situs inversus totalis. (a) A 48-year-old woman with bilateral ovarian malignancy (stars). The right ovarian vein (red arrows) crosses the midline posterior to the aorta (A) and drains into the inferior vena cava (IVC) [yellow arrow], while a prominent left ovarian vein drains directly into the left-sided IVC (blue elbow arrow). (b) A 55-year-old man with hepatocellular carcinoma (star). The IVC (yellow arrow) lies to the left of the aorta (A), with an intraluminal thrombus present in the hepatic and suprahepatic segments (black arrow).

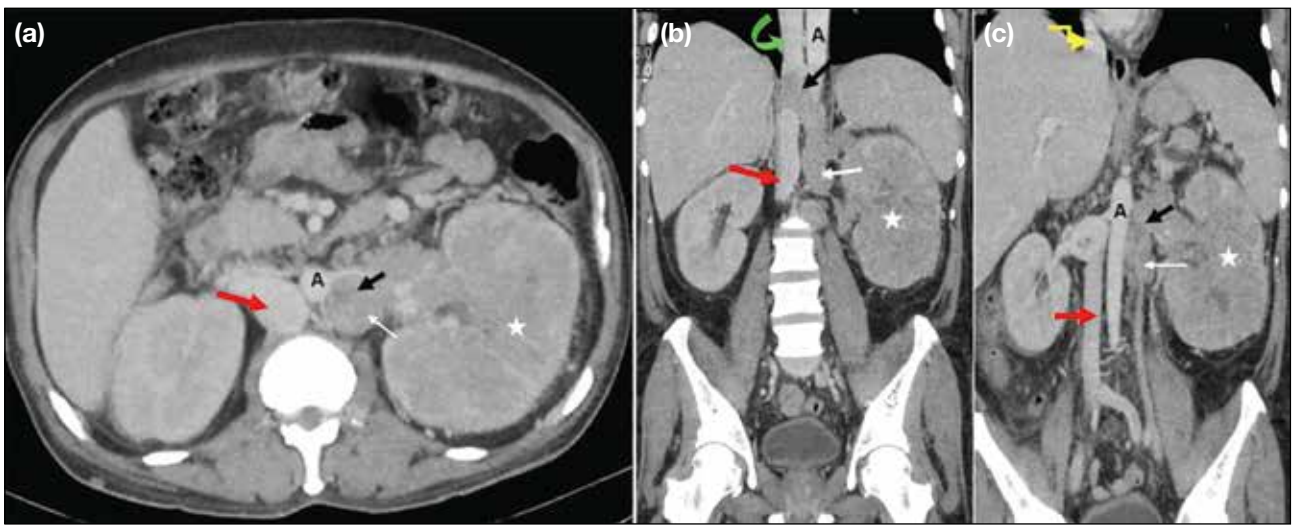

Figure 7. (a) Axial and (b, c) coronal contrast-enhanced computed tomography images of a patient with left renal cell carcinoma (stars) show a duplicated inferior vena cava (IVC) on either side of the aorta (A), with azygos continuation of the right IVC (red arrows). The left IVC (white arrows) crosses the midline and drains into the right IVC-azygos-superior vena cava pathway (green curved arrow in [b]). Tumour thrombus is present in the left renal vein and the left IVC, extending across the midline into the azygos continuation of the right IVC (black arrows). Hepatic veins drain separately into the right atrium (yellow elbow arrow in [c]).

Cancer-associated thrombosis is recognised as the most common complication of cancer and is attributed to several factors (Table 2).[7-12] Compared with the general population, patients with cancer have a 12-fold increased risk of developing venous thrombosis, as well as a significantly worse prognosis[9,10] (Figure 14). The IVC and its tributaries, especially the renal and gonadal veins, should be assessed in all abdominal malignancies

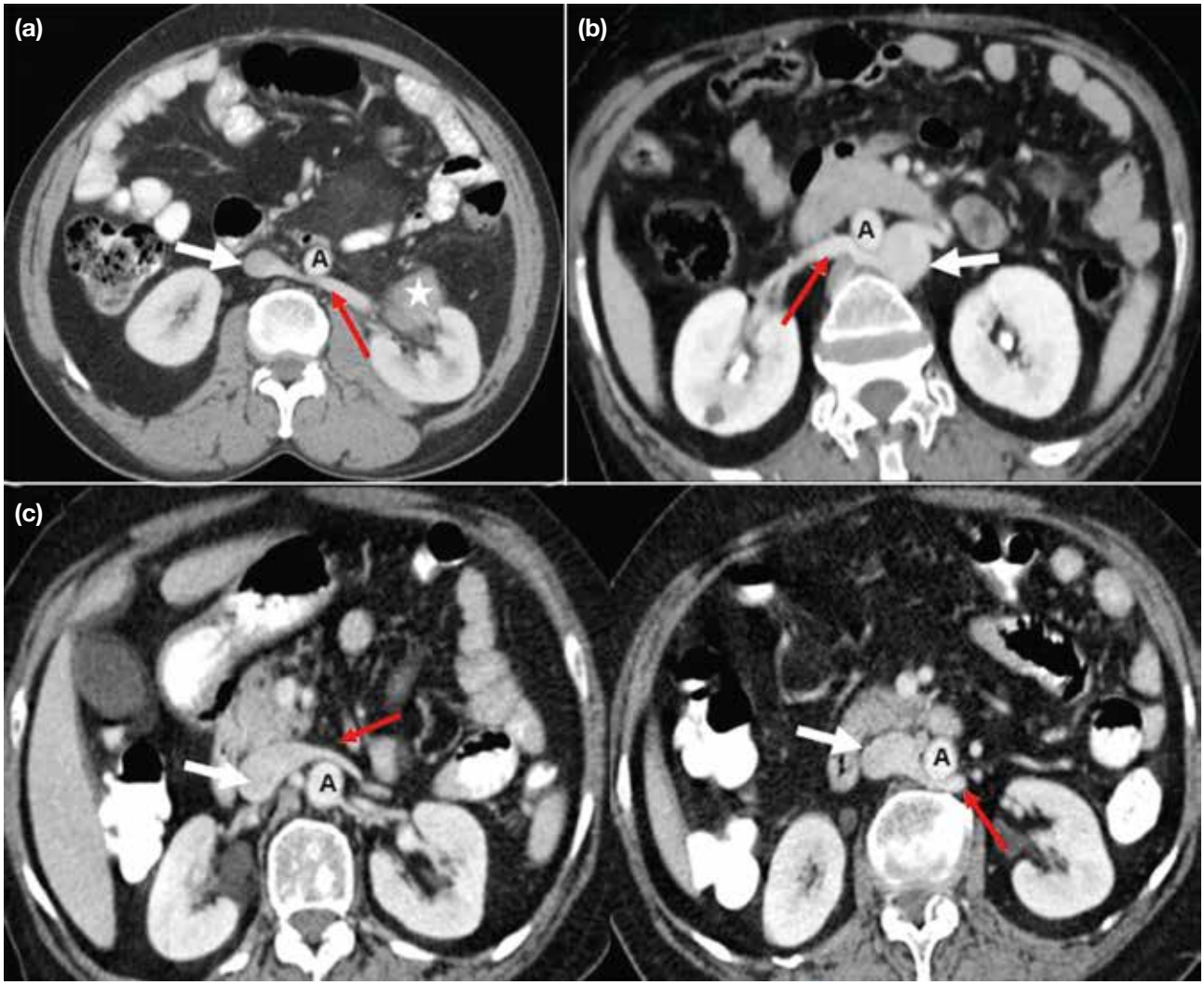

Figure 8. Contiguous axial contrast-enhanced computed tomography images showing anomalous renal veins. (a) Retroaortic left renal vein (red arrow) posterior to the aorta, draining into the normal right inferior vena cava (IVC) [white arrow] in a patient with abdominal liposarcoma (star). (b) Retroaortic right renal vein (red arrow) draining into the left IVC (white arrow). (c) Circumaortic left renal veins (red arrows) passing anterior and posterior to the aorta, draining into the right-sided IVC (white arrows).
Abbreviation: A = aorta.

to exclude thrombosis (Figure 15). Postsurgical venous thromboembolism is the leading cause of postoperative death in cancer patients, and IVC thrombosis is associated with substantial morbidity and mortality.[11,12]

Tumour thrombus results either from direct extension of the malignancy or embolisation of neoplastic cells into the abdominal veins and/or the IVC. Differentiation between bland and tumour thrombi is crucial for management: anticoagulation or catheter-directed thrombolysis is the mainstay of treatment for bland thrombus, whereas tumour thrombus may require surgical resection (Table 3).[8,13-15] In addition to tumour thrombectomy, adherent tumour thrombus invading the IVC wall necessitates en bloc excision, segmental resection, and vascular reconstruction.[15] Magnetic resonance imaging is superior to computed tomography in detecting and characterising tumour thrombus, as well as in identifying vessel wall invasion[8] (Figure 16). The extent of tumour thrombus within the IVC and the right atrium, along with vessel wall invasion, determines staging and resectability. These two factors are also independent predictors of adverse prognosis and poor survival rates in abdominal malignancies.[7,8]

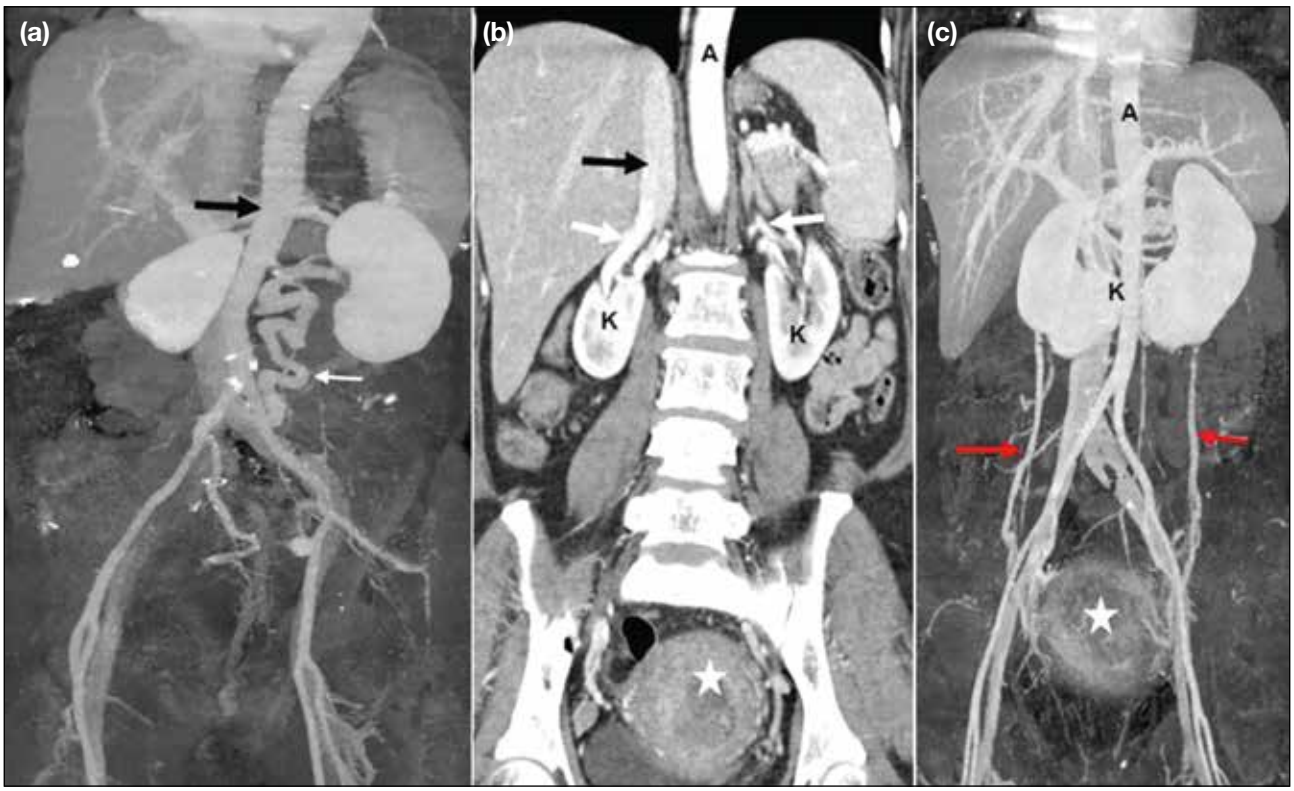

Figure 9. (a) Tortuous left renal vein draining into the left common iliac vein (white arrow) instead of the inferior vena cava (IVC) [black arrow]. (b) Anterior and (c) posterior views show 'horseshoe' kidneys (K) with vertically oriented renal veins (white arrows in [b]) and gonadal veins (red arrows in [c]) draining into the IVC (black arrow in [b]) in a patient with endometrial malignancy (stars).

Figure 10. Right adrenocortical malignancy. (a) Axial and (b) coronal contrast-enhanced computed tomography images of the abdomen show a large, heterogeneously enhancing hypoattenuating lesion (stars) invading the inferior vena cava (arrows).

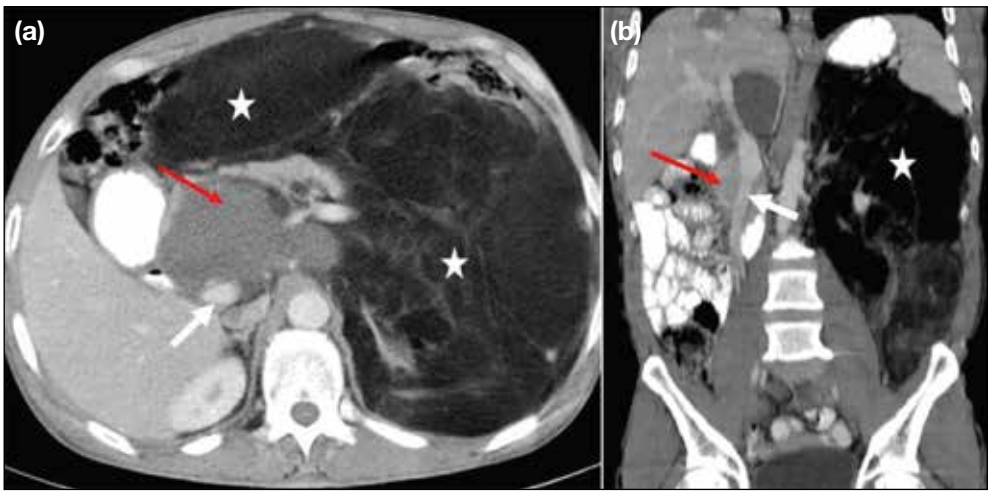

Figure 11. Retroperitoneal liposarcoma. (a) Axial and (b) coronal contrast-enhanced computed tomography images of the abdomen show large fatty component (stars) and small soft-tissue component (red arrows) encasing the inferior vena cava (white arrows).

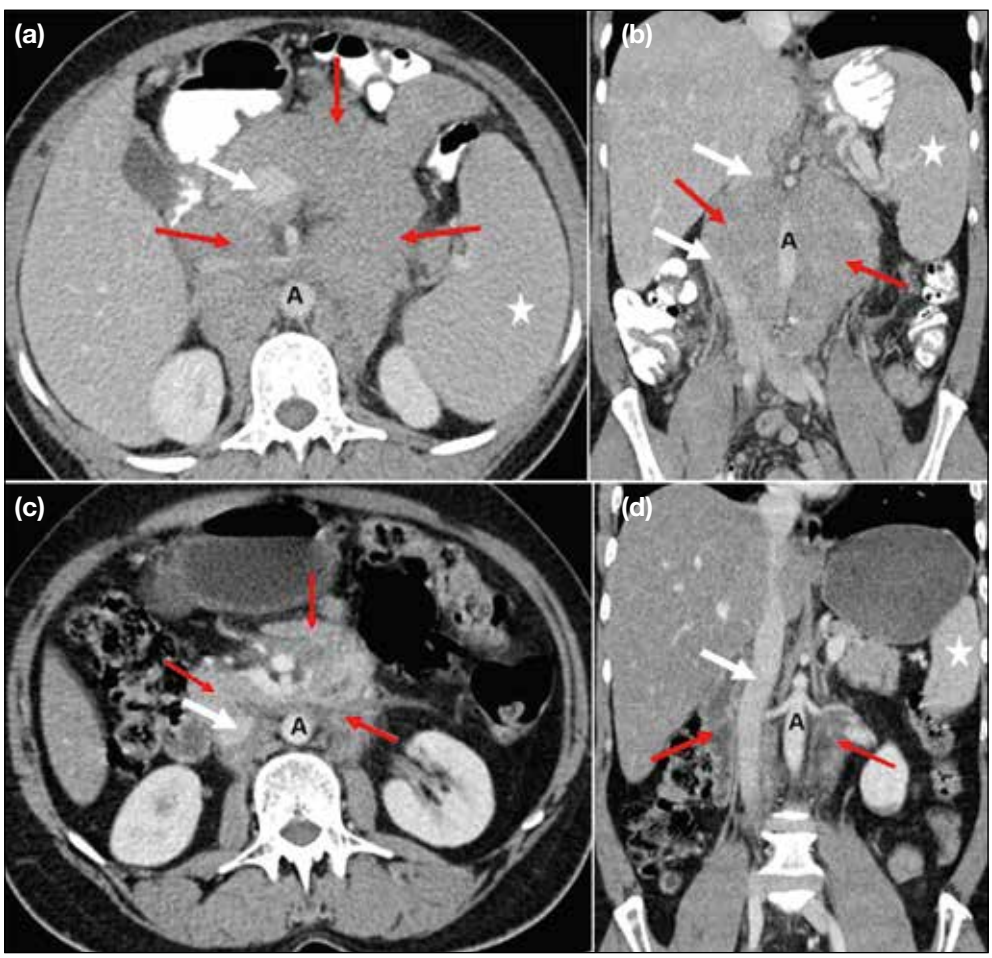

Figure 12. A 24-year-old man with lymphoma. (a) Axial and (b) coronal contrast-enhanced computed tomography images of the abdomen show splenomegaly (stars) and conglomerated nodal mass (red arrows) encasing and causing narrowing of the inferior vena cava (IVC) [white arrows], aorta, and their branches. (c, d) Corresponding post-chemotherapy images show a significant decrease in the size of the nodal mass (red arrows) and spleen (star in [d]), with expansion and visualisation of the IVC (white arrows).
Abbreviation: A = aorta.

Figure 13. Hepatocellular carcinoma (HCC) in a 56-year-old man. (a) Axial and (b) coronal contrast-enhanced computed tomography (CECT) images in the early arterial phase show contrast opacification of the aorta (A), hepatic artery, and portal vein due to an arterioportal fistula in the right lobe of the liver (black arrows). (c) Axial CECT image shows HCC (star) with thrombus in the inferior vena cava (IVC) [black arrow]. (d, e) Coronal CECT images in the venous phase show HCC (stars), along with thrombus in the portal vein (red arrow in [d]) and hepatic veins (black arrows) extending into the IVC (white arrows).

Table 2. Risk factors associated with increased incidence of thrombosis in patients with cancer.[7-12]

	Increased incidence of thrombosis
General factors	• Increasing age: >70 years (2×), >85 years (10×) • Congenital variations in anatomy of the IVC and its draining veins • Co-morbidities: infection, renal failure, lung disease, cardiac disease, and obesity • History of thromboembolism (6-7×) • Immobilisation
Cancer-associated factors	• Time period: highest risk in first year after diagnosis • High-risk primary cancer sites: pancreas, gastrointestinal tract, ovary, uterus, kidney, brain, prostate, breast, and lung • Cancer stage: greater risk with advanced-stage cancers • Cancer histology: high risk in mucin-producing adenocarcinomas • Tumour grade: high-grade (Grade 3 and Grade 4) tumours (2×) compared with low-grade tumours • Vascular tumour invasion by malignancies such as renal cell carcinoma is an independent risk factor
Cancer therapy–related factors	• Surgery: high risk in abdominopelvic and general surgeries compared with urological surgeries • Prolonged hospitalisation • Indwelling central venous catheters, IVC filters • Chemotherapy (6-7×), blood transfusions, erythropoiesis-stimulating agents • Drugs associated with thrombosis: L-asparaginase, cisplatin, tamoxifen, angiogenesis inhibitors

Abbreviation: IVC = inferior vena cava.

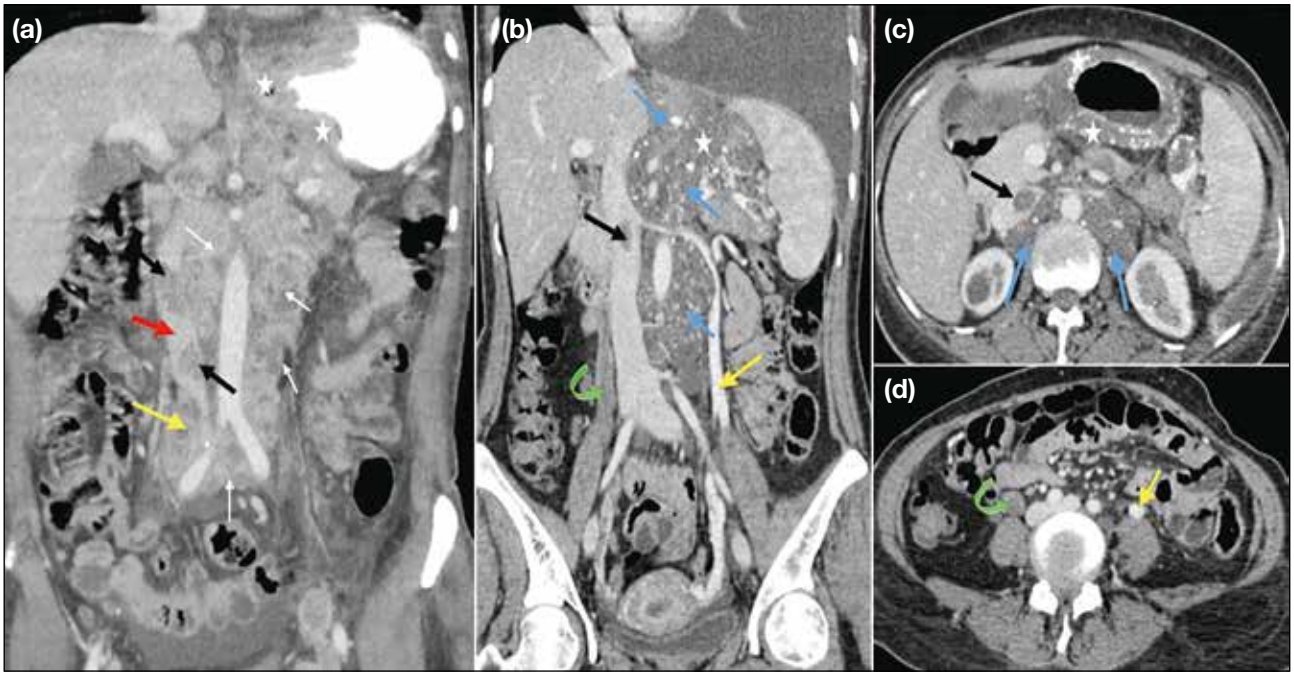

Figure 14. (a) Coronal contrast-enhanced computed tomography (CECT) image of a 56-year-old man with adenocarcinoma of the stomach shows antropyloric gastric malignancy (stars), metastatic lymph nodes (white arrows), and multiple intraluminal tumour thrombi (black arrows) in the inferior vena cava (IVC) [red arrow], with extraluminal infiltration of the IVC by right iliac lymph nodes (yellow arrow). (b) Coronal and (c, d) axial CECT images of a 42-year-old woman with mucinous adenocarcinoma of the stomach show diffuse thickening of the gastric wall (stars in [b] and [c]) and widespread metastatic lymph nodes with multiple tiny calcifications (blue arrows in [b] and [c]). A focal intraluminal thrombus in the IVC (black arrows in [b] and [c]) and a long-segment thrombus in a dilated, non-enhancing right ovarian vein (green curved arrows in [b] and [d]) are evident. The left ovarian vein (yellow arrows in [b] and [d]) is compressed by retroperitoneal lymphadenopathy.

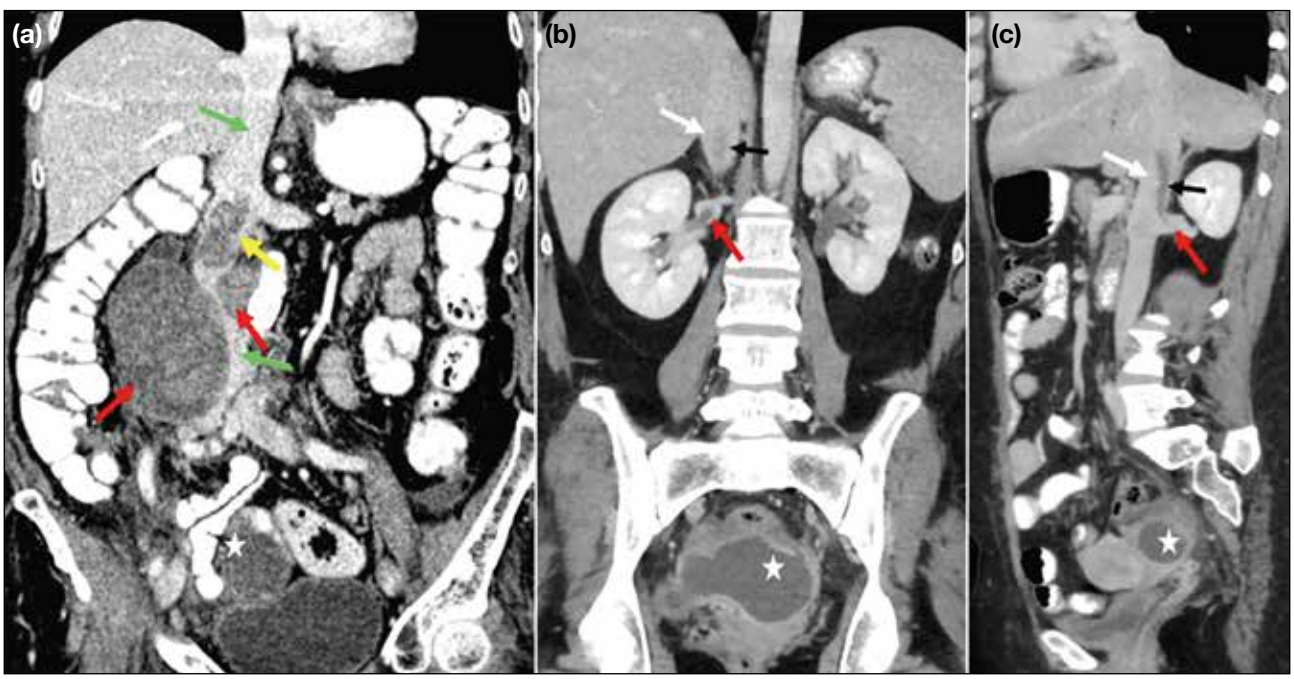

Figure 15. Two cases of ovarian cancer. (a) Coronal contrast-enhanced computed tomography (CECT) image of the abdomen of a 62-year-old patient shows right ovarian malignancy (star) with an intraluminal thrombus in the inferior vena cava (IVC) [yellow arrow] and extraluminal compression (green arrows) by enlarged lymph nodes (red arrows). (b, c) Coronal CECT images of the abdomen of a 53-year-old patient show a complex cystic lesion in the pelvis and left adnexa (stars), with bland thrombi (black arrows) in the infrahepatic IVC (white arrows) and the right renal vein (red arrows).

Table 3. Differentiating imaging features between tumour thrombus and bland thrombus.[8,13-15]

Tumour thrombus	Bland thrombus
Shows contrast enhancement on CECT and MRI	Does not enhance with contrast
May expand the vascular lumen	Does not expand the vascular lumen
Contiguous with the primary malignant lesion	Not contiguous with the primary malignant lesion
May invade the vessel wall	Does not invade the vessel wall
Shows relatively lower ADC values on MRI	May show higher ADC values on MRI
Hypermetabolic on FDG-PET/CT	Does not show FDG uptake on PET/CT

Abbreviations: ADC = apparent diffusion coefficient; CECT = contrast-enhanced computed tomography; FDG-PET/CT = fluorodeoxyglucose positron emission tomography/computed tomography; MRI = magnetic resonance imaging.

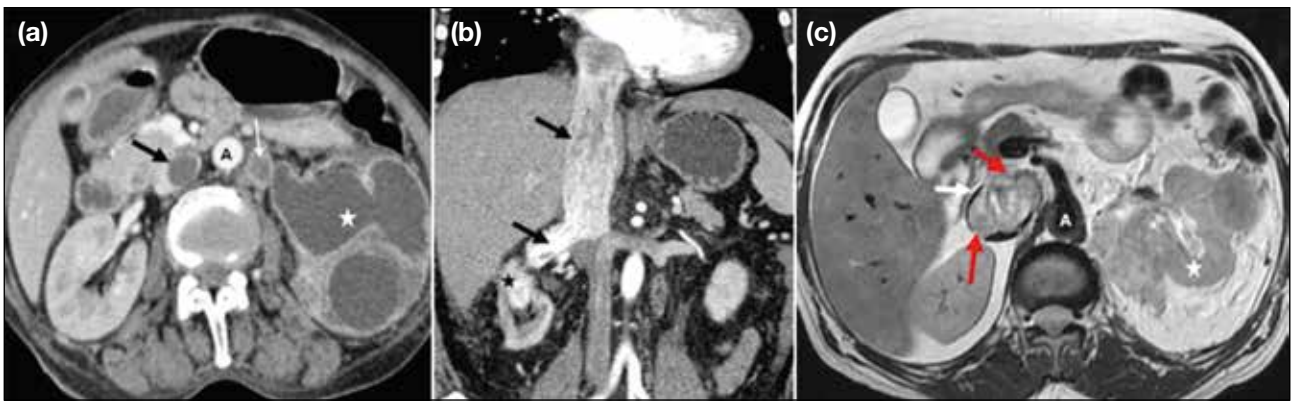

Figure 16. Renal cell carcinoma (RCC) involving the inferior vena cava (IVC) in three patients. (a) Patient 1. Axial contrast-enhanced computed tomography (CECT) image shows left RCC (star) with an enhancing tumour thrombus in the dilated left renal vein (white arrow) and a bland thrombus in the IVC (black arrow). (b) Patient 2. Coronal CECT image shows intense heterogeneous enhancement of right upper-pole RCC (star), with an enhancing tumour thrombus in the right renal vein and IVC (black arrows), extending up to the right atrium. (c) Patient 3. Axial T2-weighted magnetic resonance image shows left RCC (star) with tumour thrombus in the IVC (white arrow) focally invading the IVC wall (red arrows).
Abbreviation: A = aorta.

INFERIOR VENA CAVA IN PAEDIATRIC MALIGNANCIES

Anatomical variants in the hepatic vasculature and the IVC should be identified before segmental resection in hepatoblastoma (Figure 17). Retroperitoneal malignancies in children may involve the abdominal vasculature, including the IVC (Figure 18). Thrombosis and vascular displacement are more common in Wilms tumours than vessel encasement, whereas vascular invasion occurs more frequently in neuroblastomas[4] (Figure 19).

POSTSURGICAL COMPLICATIONS

Compression and narrowing of the IVC may occur as immediate or delayed complications in patients undergoing extensive retroperitoneal surgeries and abdominal lymph node dissections (Figure 20).

CONCLUSION

Comprehensive evaluation of the IVC and its tributaries is a critical component of pre-surgical imaging. Cancer-associated thrombosis of the IVC and abdominal veins remains underrecognised and requires a high index of clinical suspicion due to non-specific symptoms. Identifying abnormal drainage patterns and congenital variations, along with recognising intrinsic or extrinsic involvement of the IVC by abdominopelvic malignancies, is vital before undertaking major oncological surgery.

REFERENCES

1. Eitler K, Bibok A, Telkes G. Situs inversus totalis: a clinical review. Int J Gen Med. 2022;15:2437-49.
2. Bass JE, Redwine MD, Kramer LA, Huynh PT, Harris JH Jr. Spectrum of congenital anomalies of the inferior vena cava: cross-sectional imaging findings. Radiographics. 2000;20:639-52.
3. Malaki M, Willis AP, Jones RG. Congenital anomalies of the

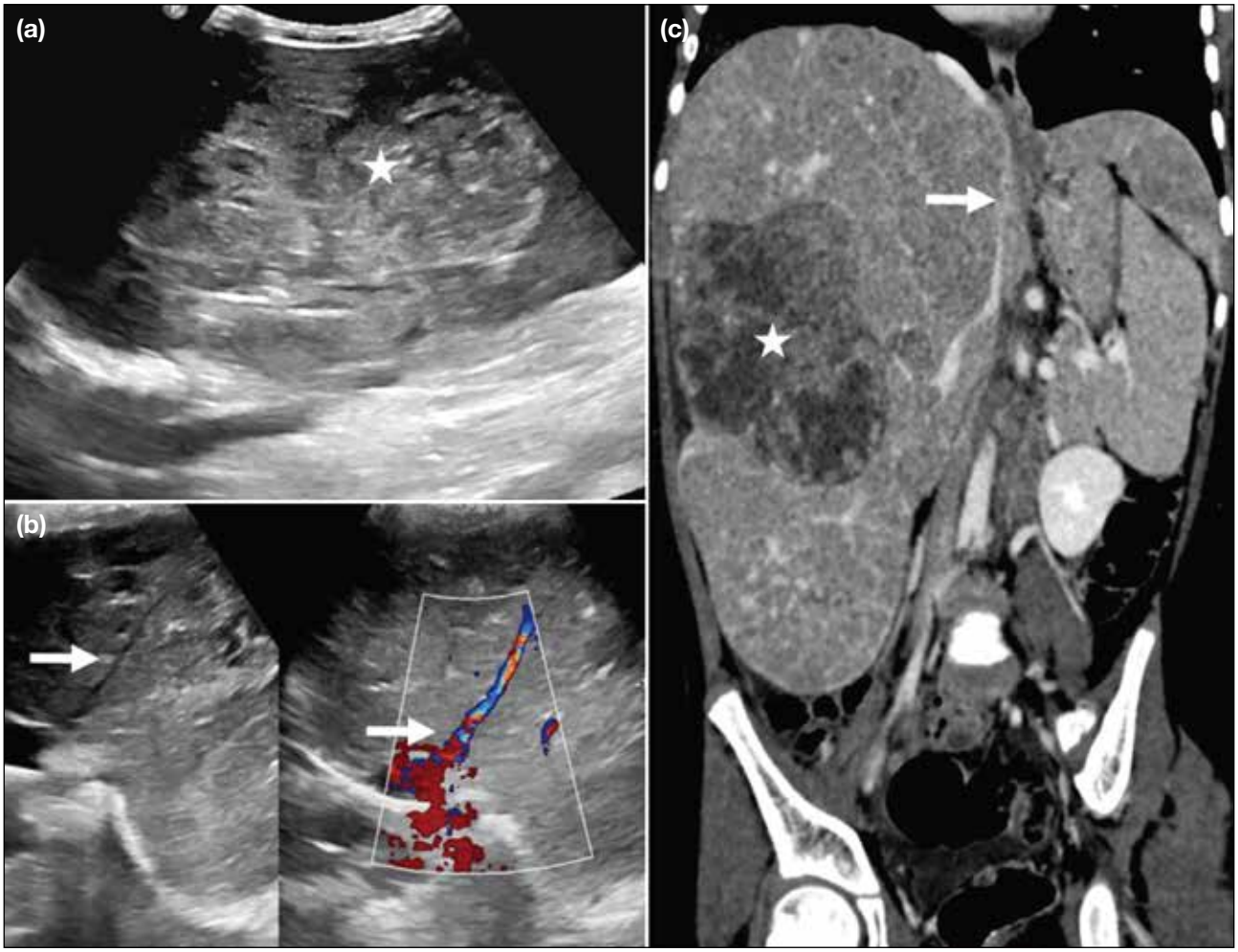

Figure 17. A 3-year-old child with biopsy-proven hepatoblastoma. (a) Greyscale and (b) colour Doppler ultrasound images show a mixed echogenic lesion (star in [a]) in the liver with narrowing of the intrahepatic inferior vena cava (IVC) [white arrows in (b)]. (c) Coronal contrast-enhanced computed tomography image of the abdomen shows a heterogeneously enhancing hypoattenuating lesion (star) in the right lobe of the liver with pronounced luminal narrowing of the intrahepatic IVC (white arrow). Hepatomegaly with patchy heterogeneous parenchymal enhancement and architectural distortion is also noted.

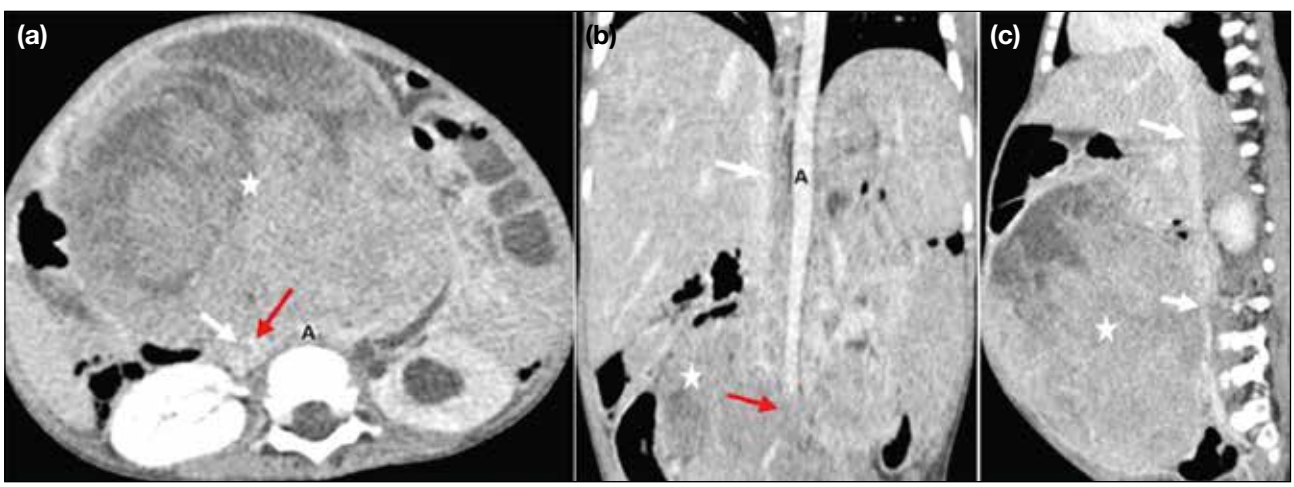

Figure 18. Retroperitoneal rhabdomyosarcoma in a 4-year-old child. (a) Axial, (b) coronal, and (c) sagittal contrast-enhanced computed tomography images show a large heterogeneously enhancing soft tissue–attenuation mass (stars) partially encasing, compressing, and narrowing the inferior vena cava (white arrows), with infiltration of the vessel wall (red arrows in [a] and [b]).
Abbreviation: A = aorta.

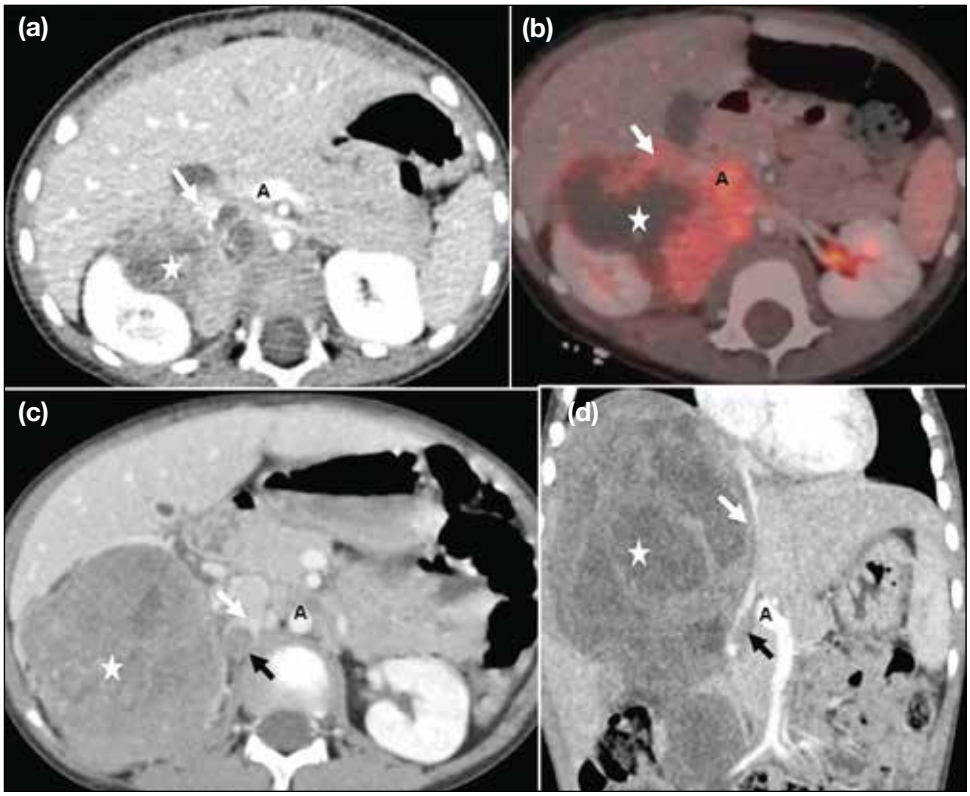

Figure 19. (a) Axial contrast-enhanced computed tomography (CECT) and corresponding (b) positron emission tomography/computed tomography fusion images of a 5-year-old child with neuroblastoma of the right adrenal gland show a hypermetabolic enhancing lesion with non-enhancing necrotic areas in the right suprarenal region (stars), encasing and infiltrating the inferior vena cava (IVC) [white arrows]. (c) Axial and (d) coronal CECT images of the abdomen of a 7-year-old child with Wilms tumour of the right kidney show a large heterogeneously enhancing tumour in the right kidney (stars), with tumour thrombus in the right renal vein (black arrows). The lesion also compresses the right lobe of the liver and causes extraluminal compression of the IVC (white arrows).
Abbreviation: A = aorta.

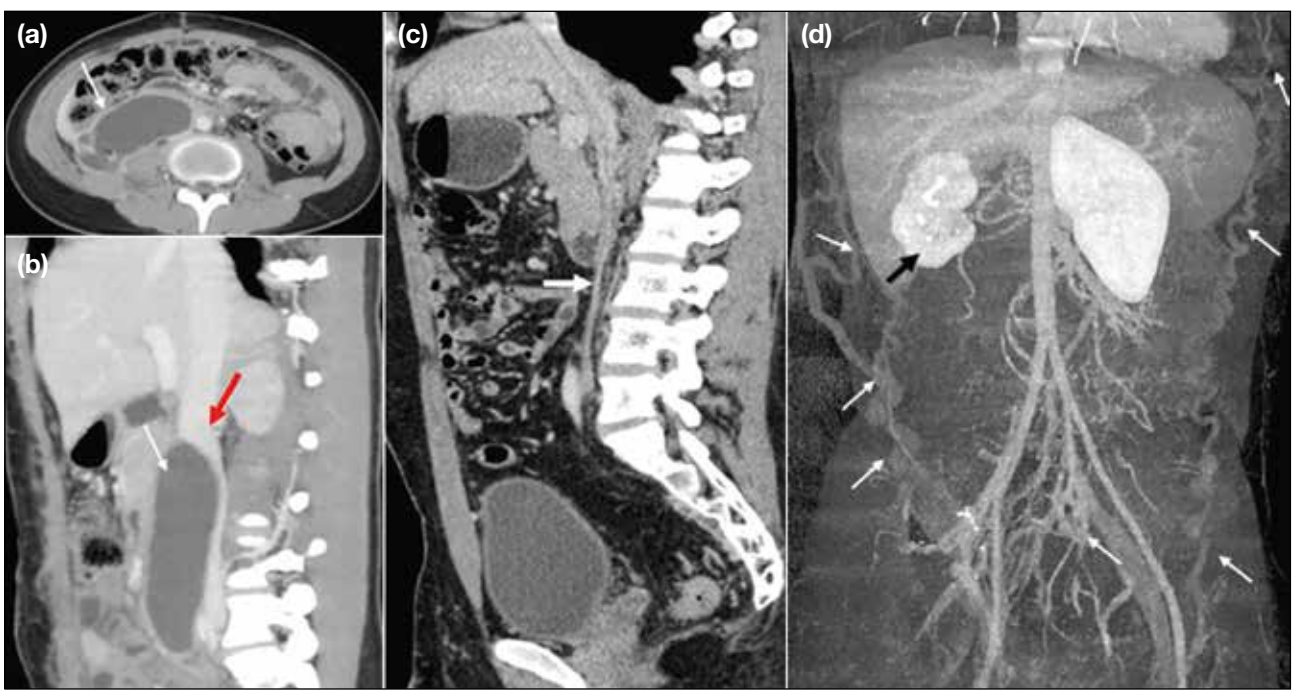

Figure 20. Immediate postsurgical complications on day 8 after para-aortic nodal dissection. (a) Axial and (b) sagittal contrast-enhanced computed tomography (CECT) images of the abdomen show a large hypodense collection (white arrows) causing extraluminal compression of the infrarenal inferior vena cava (IVC) [red arrow in (b)]. Delayed postsurgical complications in a case of carcinoma of the testis, status post-orchidectomy, and para-aortic lymphadenectomy demonstrate chronic IVC thrombosis with collateral formation. (c) Sagittal CECT image of the abdomen shows significant luminal narrowing of the IVC (white arrow). (d) Coronal maximum intensity projection image shows multiple dilated, tortuous collateral vessels in the pelvis and abdomen extending into the thoracic walls (white arrows), along with a contracted right kidney (black arrow).

inferior vena cava. Clin Radiol. 2012;67:165-71.
4. Smillie RP, Shetty M, Boyer AC, Madrazo B, Jafri SZ. Imaging evaluation of the inferior vena cava. Radiographics. 2015;35:578-92.
5. Onbaş O, Kantarci M, Koplay M, Olgun H, Alper F, Aydinli B, et al. Congenital anomalies of the aorta and vena cava: 16-detector-row CT imaging findings. Diagn Interv Radiol. 2008;14:163-71.
6. Alkhouli M, Morad M, Narins CR, Raza F, Bashir R. Inferior vena cava thrombosis. JACC Cardiovasc Interv. 2016;9:629-43.
7. Jacob T, Modgil V, Rana KK, Das S. Multiple vascular anomalies in the abdomen—a gross anatomical study. Int J Morphol. 2008;26:563-6.
8. Li SJ, Lee J, Hall J, Sutherland TR. The inferior vena cava: anatomical variants and acquired pathologies. Insights Imaging. 2021;12:123.
9. Mahajan A, Brunson A, Adesina O, Keegan TH, Wun T. The incidence of cancer-associated thrombosis is increasing over time. Blood Adv. 2022;6:307-20.
10. Abdol Razak NB, Jones G, Bhandari M, Berndt MC, Metharom P. Cancer-associated thrombosis: an overview of mechanisms, risk factors, and treatment. Cancers (Basel). 2018;10:380.
11. Agnelli G, Bolis G, Capussotti L, Scarpa RM, Tonelli F, Bonizzoni E, et al. A clinical outcome–based prospective study on venous thromboembolism after cancer surgery: the @RISTOS project. Ann Surg 2006;243:89-95.
12. Teter K, Schrem E, Ranganath N, Adelman M, Berger J, Sussman R, et al. Presentation and management of inferior vena cava thrombosis. Ann Vasc Surg. 2019;56:17-23.
13. Akin O, Dixit D, Schwartz L. Bland and tumor thrombi in abdominal malignancies: magnetic resonance imaging assessment in a large oncologic patient population. Abdom Imaging. 2011;36:62-8.
14. Catalano OA, Choy G, Zhu A, Hahn PF, Sahani DV. Differentiation of malignant thrombus from bland thrombus of the portal vein in patients with hepatocellular carcinoma: application of diffusion-weighted MR imaging. Radiology. 2010;254:154-62.
15. Adams LC, Ralla B, Bender YY, Bressem K, Hamm B, Busch J, et al. Renal cell carcinoma with venous extension: prediction of inferior vena cava wall invasion by MRI. Cancer Imaging. 2018;18:17.